A SPHERICAL LAMELLAR GRATING INTERFEROMETER FOR AIRBORNE ASTRONOMICAL OBSERVATIONS OF FAR INFRARED OBJECTS

J.L. Pipher, M.P. Savedoff and J.G. Duthie

*University of Rochester

Department of Physics and Astronomy

Rochester, New York 14627

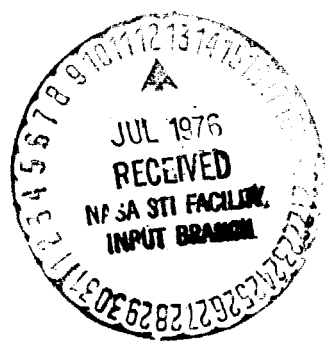

Abstract

A lamellar grating has been developed to be used for very far infrared observations on the Gerard P. Kuiper Airborne Observatory. The design characteristics and performance during laboratory testing and initial observations of Jupiter at wavelengths between 50 and 500μ are presented.

I. Introduction

We have developed a lamellar grating interferometer for use on the Gerard P. Kuiper Airborne Observatory. This Observatory consists of a 91cm., f/13.5 Cassegrain focus telescope mounted in a C-141 aircraft dedicated to infrared astronomy and operated by the National Aeronautics and Space Administration. The aircraft operates at altitudes of 40,000 feet and above, where residual precipitable water vapor is typically below 20μ and frequently below 10μ. The observatory is thus ideal for studying extremely far infrared astronomical objects at wavelengths in excess of 50μ. In this wavelength range most observations utilizing sensitive detectors such as gallium doped germanium bolometers will be detector noise limited and so that Fellgett's advantage of Fourier transform spectroscopy can be fully realized. In fact other noise sources associated with the atmosphere-aircraft-telescope system dominated, and for this case Fellgett's advantage is also operative. Our interferometer was designed specifically to study this part of the very far infrared spectrum. The instrument, which utilizes spherical lamellar facets (such as those described by Hansen and Strong[1]) has been used to obtain spectra of several astronomical bodies. In this paper we present a description of the instrument and discuss its response to a laboratory far infrared source and to Jupiter as viewed from the Airborne Observatory.

II. Instrument Design

In the spectral range of interest the advantage of the lamellar grating interferometer (which employs wavefront division) over the Michelson interferometer (which employs amplitude division) has been discussed by several authors including Richards[2] and Milward[3]. The lack of really

suitable materials for use as beam splitters over a wide spectral range and the further disadvantage of losing half the available signal from what is usually rather a weak source dictates against the single detector Michelson interferometer, and the ideal double beam Michelson interferometer exhibits $\sqrt{2}$ times the noise.

Strong and Vanasse[4] have discussed in some detail the theory of lamellar grating interferometers. In these devices modulation results from relative motion (along the optical axis) of two sets of parallel, intermeshing facets forming a grating surface. Each set of facets give rise to a diffracted beam and furthermore these beams interfere as a result of the relative displacement of two sets of reflecting surfaces. The zeroth order of the diffraction pattern is modulated as $\cos^2 \pi\nu\Delta$ where Δ is the optical path difference between the sets of facets. Ideally, all other <u>even</u> order diffraction patterns are absent and the odd orders are modulated as $\pm \cos^2 \pi\nu\Delta$. To optimize the modulation we exclude all but the zeroth order by limiting the exit and entrance aperture sizes. The maximum wave number ν_{max} that can be accepted will depend on the focal length of the collimating optics, f, the exit aperture size, w, and the distance between the centers of alternate facets, a , and is given by

$$\nu_{max} = f/aw \ .$$

Further constraints restrict the choices of w and a. The exit aperture should be large enough to optimize throughput and in particular to exceed the diffraction limit of the telescope at the longest wavelengths, yet block first order spectra. The grating spacing also has to be large enough to ensure that cavity effects do not occur. These effects result when wavelengths approaching

the widths of the facets, a, are involved. In this case propogation of the radiation to the rear set of facets involves wave guide modes with resultant phase shifts which limit the instrumental resolution for unpolarized radiation. To be consistent with these considerations the detection system included a filter to reject $\nu > 200\text{cm}^{-1}$.

The interferogram ($I(\Delta)$) of a source, obtained by stepping the lamellar grating system, leads to an output of the form

$$I(\Delta) = \int_0^\infty S(\nu)[1 + \cos(2\pi\nu\Delta)]\, d\nu$$

$$= \frac{I(0)}{2} + \int_0^\infty S(\nu)\cos(2\pi\nu\Delta)d\nu$$

where $S(\nu)$ is the spectrum of the source. Hence the desired spectrum is obtained by computing the cosine Fourier Transform of $[I(\Delta) - \frac{I(0)}{2}]$ namely $S(\nu) = 4\int_0^\infty [I(\Delta) - \frac{I(0)}{2}] \cos(2\pi\nu\Delta)d\Delta$ and is calculated by the Cooley-Tukey Fast Fourier transform algorithm[5]. Standard usage of this algorithm incorporates discrete sampling up to a maximum optical path difference, Δ_{max} and suitable apodization.

A further advantage occurs if the lamella are machined to a spherical surface rather than plane. In this case, as discussed by Hansen and Strong, the grating is self-collimating and the need for entrance and exit collimating mirrors is eliminated. The radius of curvature of the grating was chosen to be consistent with the f-ratio of the telescope and with the diameter of the grating itself. This latter size was chosen to give a reasonable number of facets consistent with the size considerations discussed above and with the constraint that shadowing of the rear facets by the forward facet be less than 1%. Shadowing effects arise because one must operate the grating slightly off normal incidence in order to separate

the entrance and exit apertures.

The grating itself is shown in Plate (1). It is 9cm. in diameter and the two sets of facets are machined out of brass to a concave spherical surface of 1.24 meters radius of curvature. Fabrication from brass ensured relatively easy machining and polishing of the surfaces. Gold plating of the finished surfaces was found to increase slightly their far infrared reflectivity, and also prevents surface deterioration.

The relative alignment of the two sets of facets (stationary and moving) was achieved by means of a specially designed positioning device which controlled the orientation of the fixed set of facets by means of three screws. The moving set of facets is mounted rigidly on a piston arrangement attached to an Aerotech ATS 301 translation stage. The stage is driven by a pulsed stepping motor with a minimum 0.0001" displacement. Each facet is approximately 0.76cm wide and the interfacet spacing was chosen to be .01cm to minimize loss of the reflecting area consistent with free relative motion.

Figure (1) shows the optical arrangement. The entrance aperture was located at the prime focus of the telescope. A dichroic beam splitter was used to reflect the infrared signal but transmitted the visible light thereby allowing us to monitor the field of view. An additional plane mirror was necessary to fold the optical path in such a way as to package the instrument consistent with mechanical limitations on the support and balance of the telescope. This mirror reflected both the incident and reflected beam from the grating. The optical axis of the grating was at 4° to the axis of the incident radiation. The exit aperture was defined by the cooled filters preceding the field mirror feeding the bolometer. The detector itself was a gallium doped germanium bolometer supplied by

Infrared Laboratories Incorporated. In laboratory testing, a chopping wheel located at the entrance aperture was used to modulate the radiation from a Barnes Engineering blackbody placed immediately behind it. In flight, modulation was achieved by means of an articulating secondary on the telescope. A throw of 8' arc ensured that the detector looked alternately at the source and at an adjacent region of the sky beyond the diffraction limit of the telescope. The entrance aperture was ~ 2' which is equivalent to the diffraction limit of the telescope at 250μ. The response of the bolometer was preamplified at the dewar and then synchronously detected by means of a lock-in amplifier. The overall system NEP as measured in the laboratory was $< 2 \times 10^{-12}$ watts/$Hz^{1/2}$. We were never able to remove completely the attenuation by telluric water vapor in the laboratory, hence the quoted NEP is an upper limit. The maximum range of the translation stage is 2.5cm, leading to an overall optical path difference of 5cm. which corresponds to a limiting resolution of $0.2cm^{-1}$.

Figure (2) shows schematically the optical and electronic system. Infrared radiation from the star passes through the telescope whose secondary is articulated at a 12Hz rate. The radiation continues to the lamellar grating and then to the bolometer by the optical path indicated in Figure (1). The output of the lock-in amplifier is fed to both a paper tape printer for permanent recording and to an A/D converter controlled by the HP 2100 computer on board the aircraft.

Control of the grating is handled by a step driven controller which automatically sequences the motor with the option of manually interrupting the sequence. The operator selects the step size (in increments of 0.0001") at which the interferogram is sampled, the dwell time at each sampling point and the maximum displacement required for each interferogram. The

controller also provides gate pulses to ensure that the paper tape printer and the computer respond only during times when the signal will have stabilized at a given grating setting. The paper tape printer records only once at each grating setting while the computer samples the lock-in amplifier every 100 milliseconds during the same time. The 100 msec sampling time in the flight system, together with the 300msec time constant of the lock-in amplifier, resulted in readings recorded on tape which are not entirely independent. A magnetic tape recorder stores all these measurements together with real time computed averages of interferograms and Fast Fourier transforms of the interferograms. In addition the inflight computer records auxilliary flight and housekeeping information and provides on-line information regarding the observations, including hard copies of the fast Fourier transforms for quick look purposes. Eventually the magnetic tape was analyzed at our own computing center where any necessary data "massaging" was applied and final reductions were made.

III. Results

Figures (3) and(4) show two spectra taken in the laboratory. The crosses and dots refer to unapodized and apodized spectra respectively. The first curve shows an unpurged spectrum and the effects of atmospheric absorption result in a strongly wavelength dependent structure. The resolution of the feature at 161cm^{-1} approached the anticipated resolution of 4.75cm^{-1} for this run. By comparison the second spectrum shows the result of purging the approximately 2.5m optical path with dry nitrogen thereby removing most of the water vapor. The gross changes testify to the high degree of absorption by rotational excitation of the water vapor in the first spectrum. That the purging was incomplete is shown by the

residual absorption features of the spectrum in figure (4).

During the night of November 7, 1965 U.T. we obtained several extended observations of Jupiter, Mars, Saturn, and the Kleinmann-Low object in the Orion Nebula. In particular we obtained three interferograms of Jupiter and a typical raw spectrum calculated from one of these is shown in figure (5). The general features of the spectrum are present in all three observations.

Many of the absorption features are identified with rotation bands of H_2O and are probably telluric. These include strong features at 149.1cm^{-1}, 150.6cm^{-1}, 132.7cm^{-1}, 127cm^{-1}, 122.0cm^{-1}, 120.7cm^{-1}, 99.0cm^{-1}, 88.0cm^{-1} and 73.2cm^{-1} [6,7] some of which are blended at the best resolution employed on this flight, 3 cm^{-1}. The spectra of Mars taken on the same night showed the same absorption lines. Complete analysis of these data will be reported in subsequent papers.

IV. Summary

The lamellar grating interferometer on the Gerard P. Kuiper Airborne Observatory has been shown to be a reliable useful system for the study of far infrared astronomy in the range 50-800μ. Its self-collimating allows for the efficient operation with the minimum of auxiliary optics.

The authors wish to thank M. Toporek, S. Varlese, R. Lerner, and J. Krassner for their varied assistance in this research. Pan Monitor Inc. designed the mechanical support structure, and G. Lanpher designed and constructed the electronic sequence controller. We particularly wish to thank the staff of the NASA-Ames Airborne Sciences division and the ADAMS group for their enthusiastic support and assistance during our flight series. Support for this work was provided by NASA under grant NGR33-019-127.

Bibliography

1. Hansen, J.P. and Strong, J. Aspen International Conference on Fourier Spectroscopy, 1970, p. 215.
2. Richards, P.L., 1964, JOSA 54, 1474.
3. Milward, R.C., 1969, Infrared Physics 9, 59.
4. Strong, J. and Vanasse, G.A., 1960, JOSA 50, 113.
5. Cooley, J.W. and Tukey, J.W., 1965, Mathematics of Computation 19, 287.
6. Hall, R.T. and Dowling, J.M., 1967, J. Chem. Phys. 47, 2454.
7. Randall, H.M., Dennison, D.M., Ginsburg, N. and Weber, L.R., 1937, Phys. Rev. 52, 160.

Figure Captions

Plate 1. Photograph showing the lamellar grating mounted in its housing. The two sets of facets and the adjustment screws for the fixed set are clearly visible.

Figure 1. The optical arrangement for the lamellar grating interferometer.

Figure 2. Flow Chart of the Optical and Electronic System.

Figure 3. Unpurged Spectrum of 1000°K blackbody source. Solid line joining dots represents spectrum with triangular apodization. Crosses are the unapodized spectrum. Resolutions of feature near 163 cm^{-1} are shown. Theoretical apodized resolution for the length of run used is 4.75cm^{-1}. Selected strong water vapor transitions shown by vertical arrows.

Figure 4. Purged Spectrum of 1000°K blackbody source.

Figure 5. Raw Spectrum of Jupiter, at 3.2cm^{-1} resolution obtained Nov. 1975.

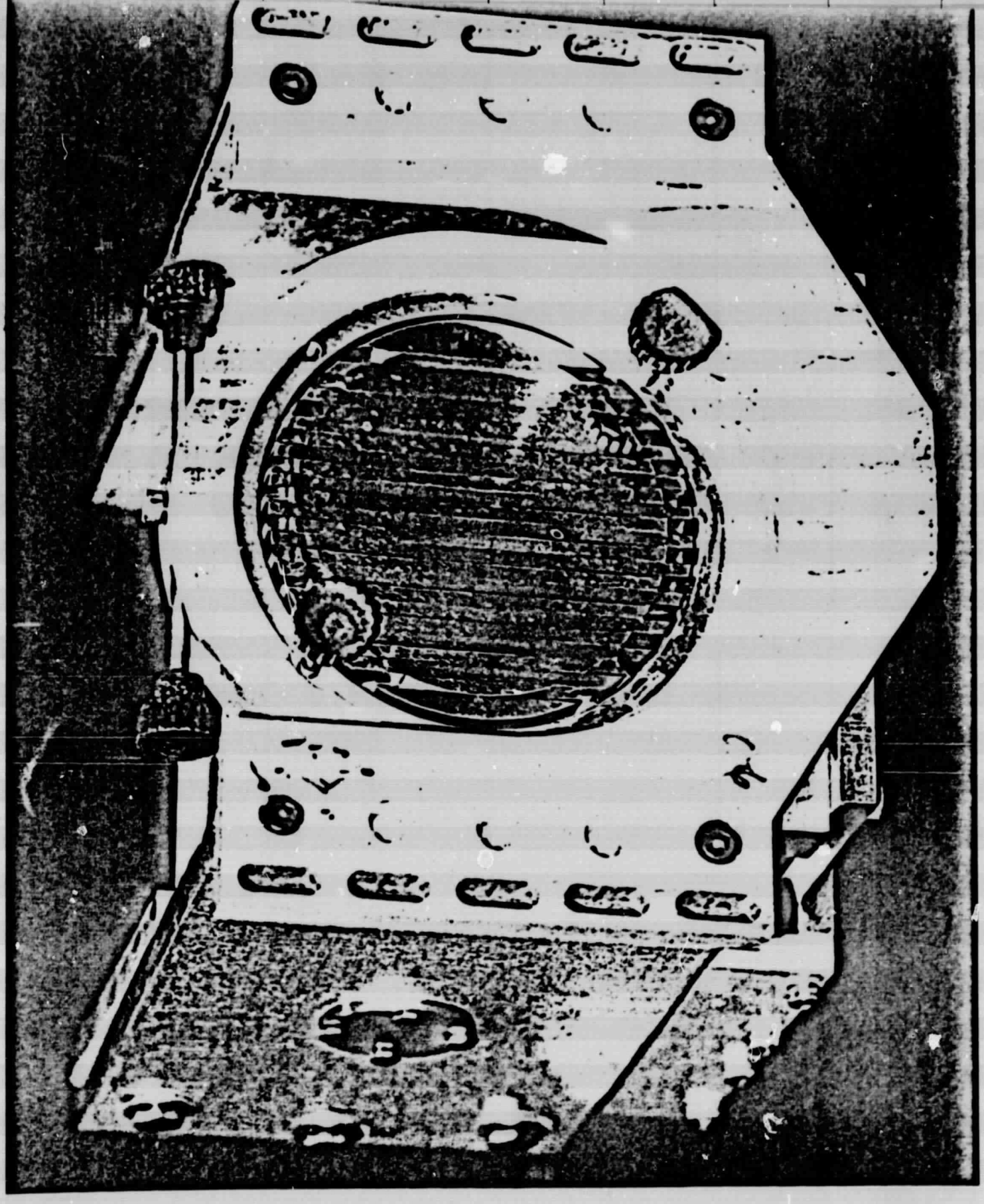

Plate 1

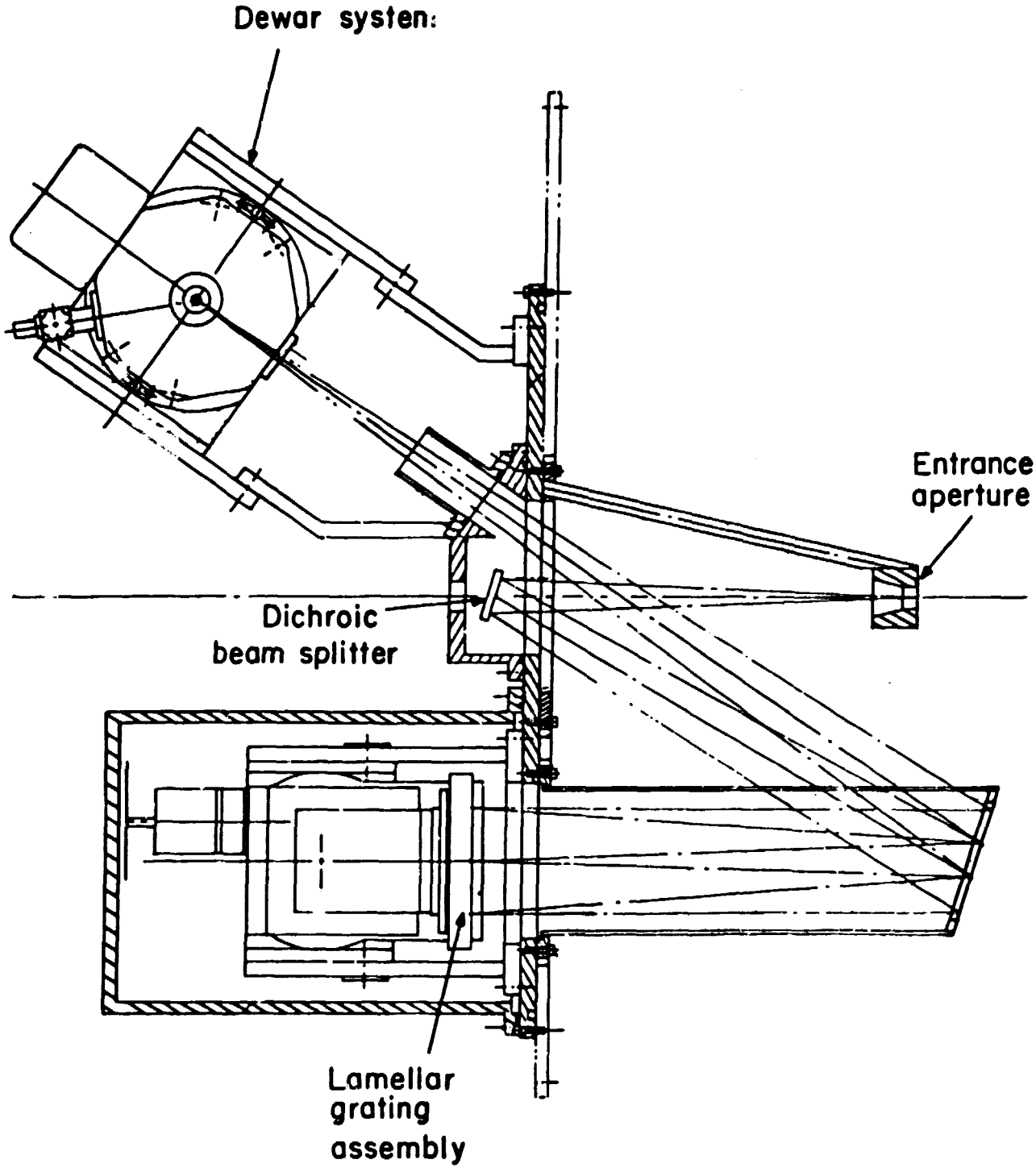
Dewar system
Entrance aperture
Dichroic beam splitter
Lamellar grating assembly

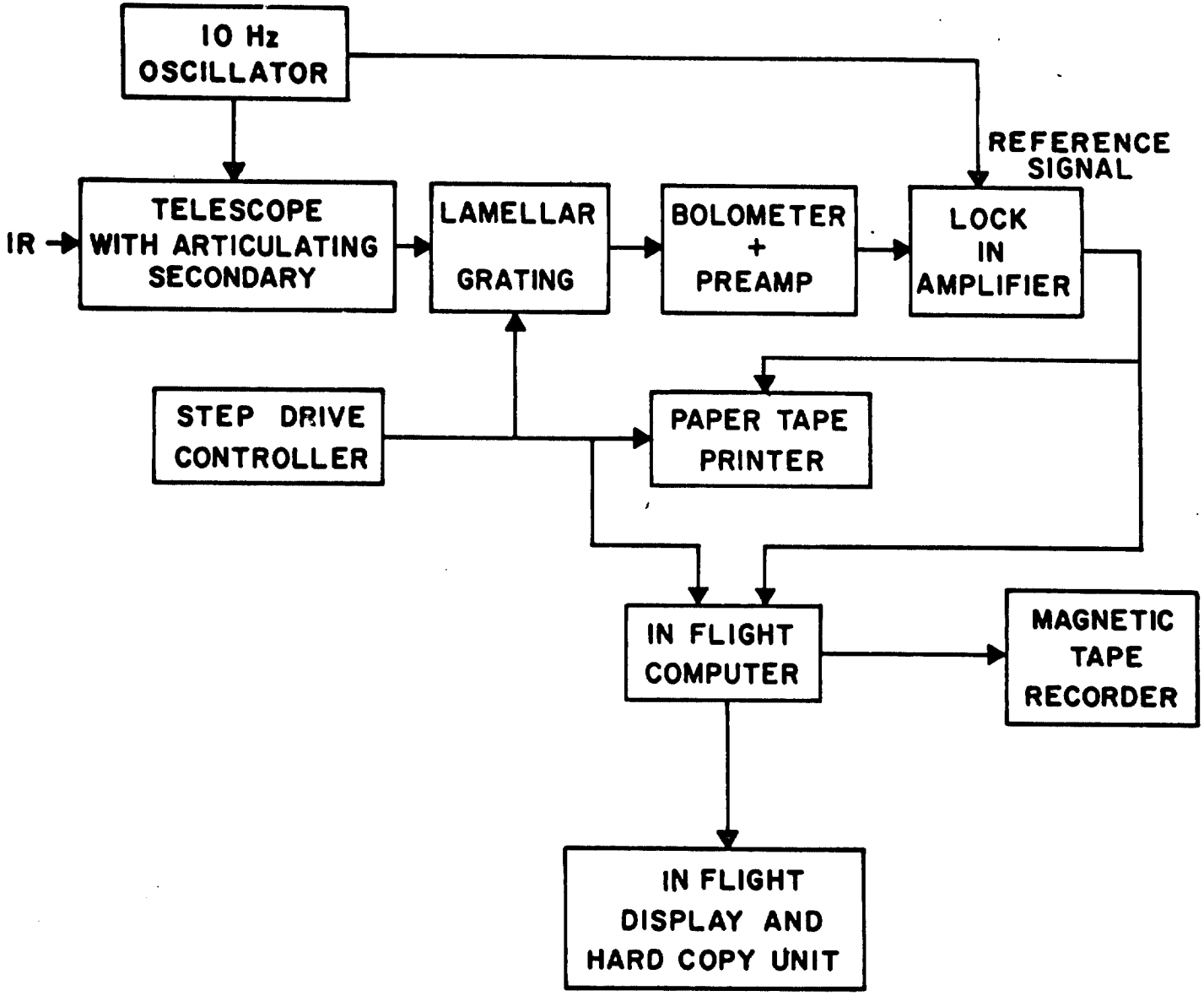
10 Hz
OSCILLATOR
REFERENCE
SIGNAL
IR
TELESCOPE
WITH ARTICULATING
SECONDARY
LAMELLAR
GRATING
BOLOMETER
+
PREAMP
LOCK
IN
AMPLIFIER
STEP DRIVE
CONTROLLER
PAPER TAPE
PRINTER
IN FLIGHT
COMPUTER
MAGNETIC
TAPE
RECORDER
IN FLIGHT
DISPLAY AND
HARD COPY UNIT

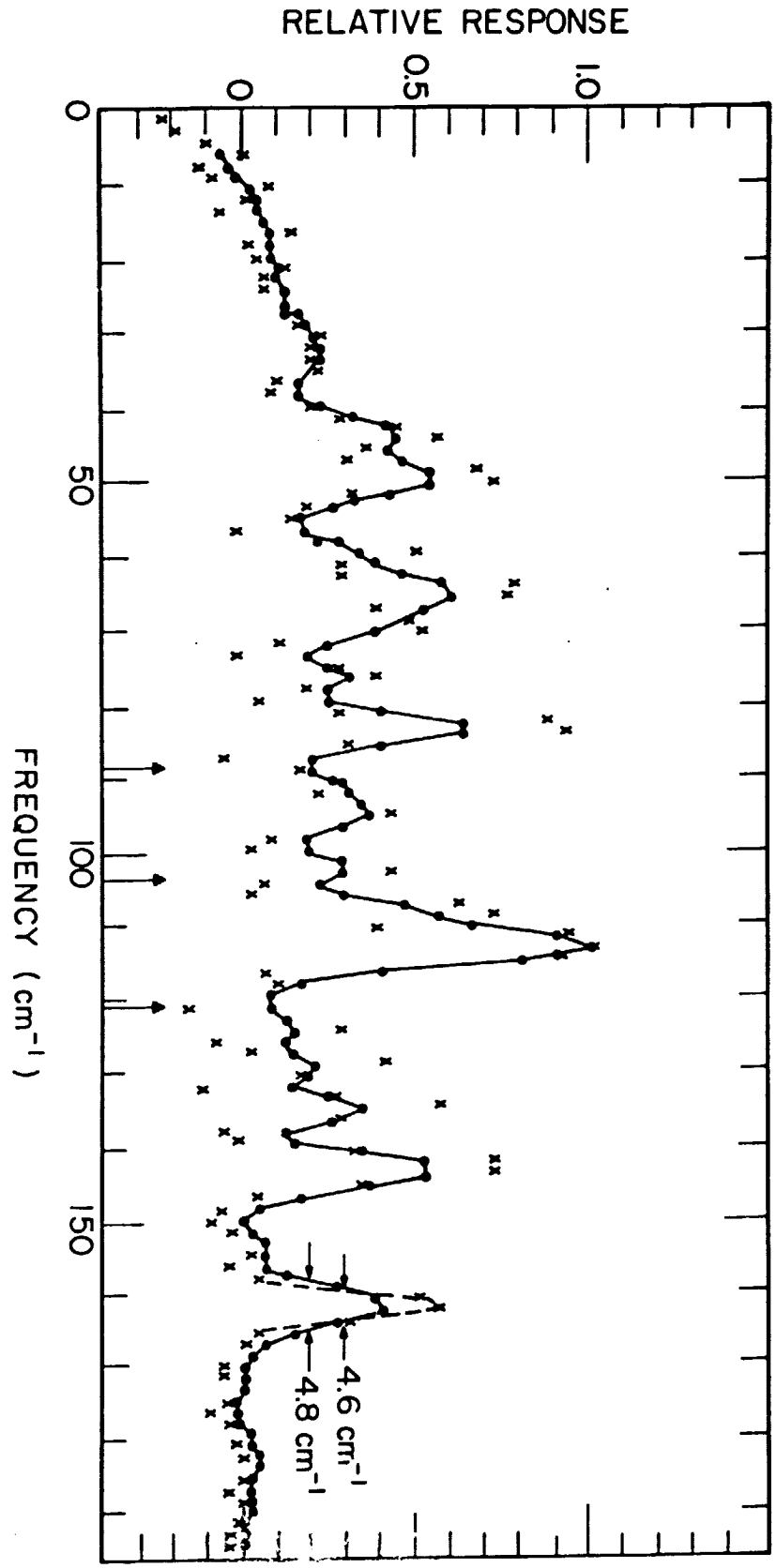
RELATIVE RESPONSE
0
0.5
1.0
0
50
100
150
FREQUENCY (cm⁻¹)
4.6 cm⁻¹
4.8 cm⁻¹

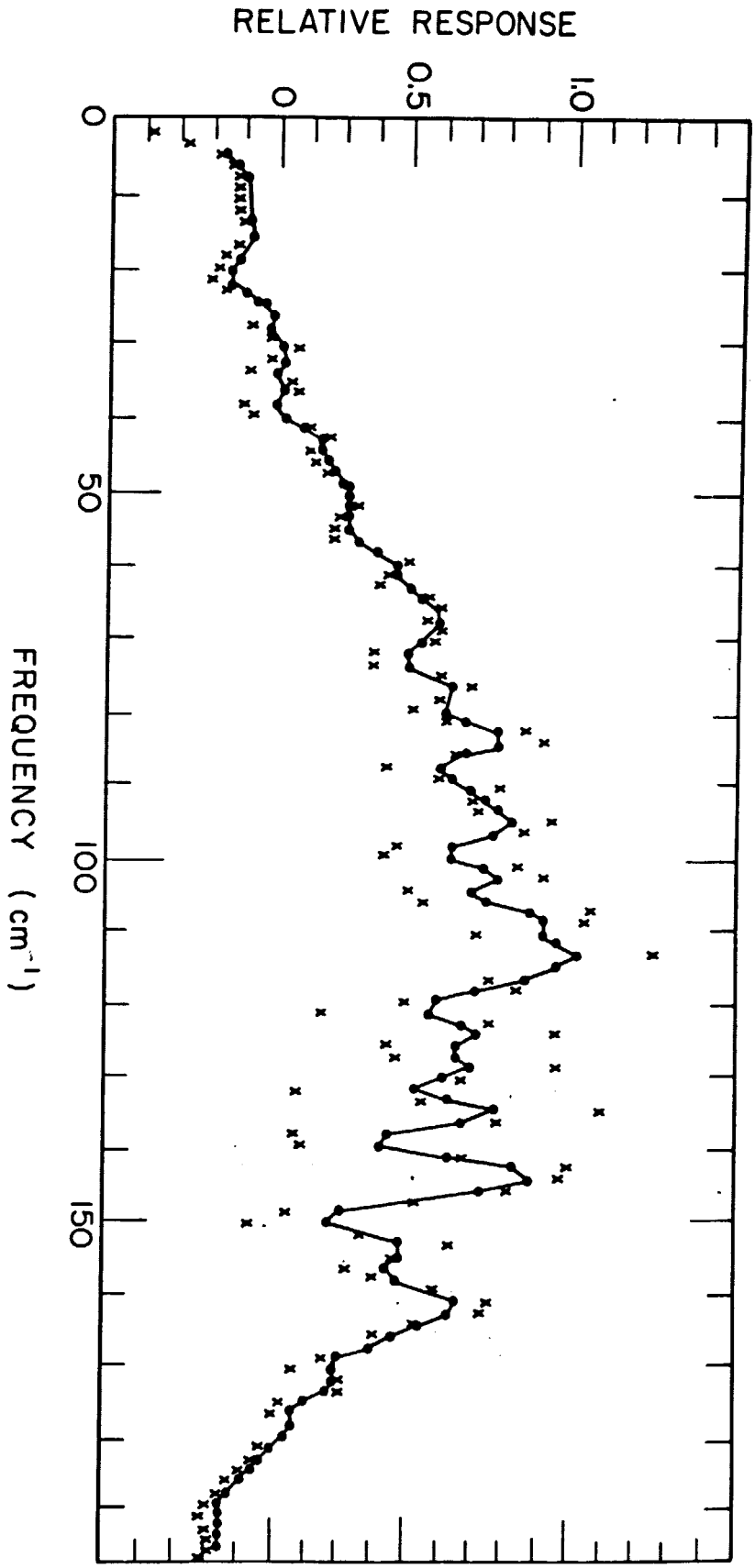
RELATIVE RESPONSE
0
0.5
1.0
0
50
100
150
FREQUENCY (cm⁻¹)

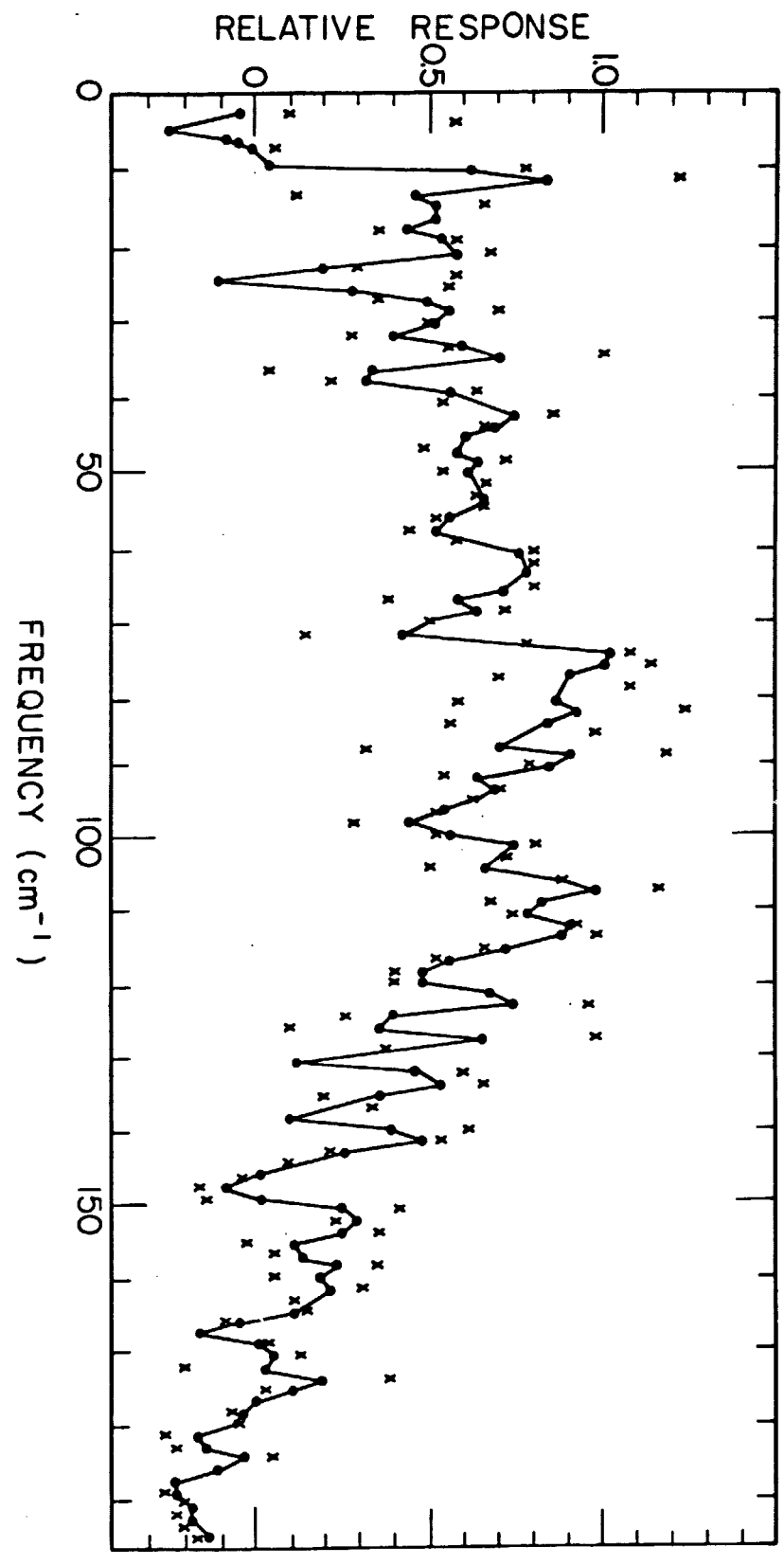
RELATIVE RESPONSE
0
0.5
1.0
0
50
100
150
FREQUENCY (cm⁻¹)